J. Anat. (1995) 187, pp. 361–368, with 3 figures Printed in Great Britain

Stereological methods for estimating the functional surfaces of the chiropteran small intestine

A. N. MAKANYA[1], T. M. MAYHEW[2] AND J. N. MAINA[1]

[1] *Department of Veterinary Anatomy, University of Nairobi and* [2] *Department of Human Morphology, University of Nottingham, UK.*

(*Accepted 7 March 1995*)

ABSTRACT

A tissue sampling protocol has been devised for studying the functional surfaces of chiropteran small intestine and drawing comparisons within and between species. The goal was to obtain minimally biased stereological estimates of villous and microvillous surface areas and the numbers of microvilli. The approach is illustrated using the intestines of 3 bats (from frugivorous and entomophagous groups) and is based on the use of vertical sections and cycloid test arcs. A sampling scheme with 3 levels was employed. At level 1 (macroscopy), primary mucosal area was estimated from intestinal length and perimeter. Amplification factors due to villi were estimated at level 2 (light microscopy, LM) whilst microvillous amplifications were estimated at level 3 (transmission electron microscopy, TEM). The absolute surfaces, lengths and diameters of microvilli were used to calculate packing densities and absolute numbers. Estimated villous surface areas of the entire small intestine were 44.4 cm^2 (*Miniopterus inflatus*, entomophagous), 410 cm^2 (*Epomophorus wahlbergi*, frugivorous) and 237 cm^2 (*Lisonycteris angolensis*, frugivorous). Corresponding microvillous surface areas were 0.11, 1.69 and 1.01 m^2 whilst the numbers of microvilli per intestine were 4.5, 23.4 and 8.8×10^{11}. When normalised for body weights, microvillous surfaces were 122, 246 and 133 cm^2/g respectively. The functional surfaces of the fruit bat appear to be more extensive than those of the entomophagous bat.

Key words: Bat; intestine; villi; microvilli.

INTRODUCTION

Bats are unique amongst mammals in their capacity for active flight (Greenhall & Paradiso, 1968; Wimsatt, 1970; Thomas & Suthers, 1972; Dawson, 1975; Thomas, 1975, 1980; Yalden & Morris, 1975; Jurgens et al. 1981). Active flight is energy-expensive and, for bats, the metabolic cost is comparable to that in birds (Thomas & Suthers, 1972; Tucker, 1972; Carpenter, 1975). The highest metabolic rates are essentially the same as those of birds of comparable body mass but 2 or 3 times greater than in comparable exercising terrestrial mammals (Thomas, 1975, 1984). Bats display respiratory (Maina et al. 1982, 1991) and cardiovascular (Jurgens et al. 1981; Ayettey et al. 1991) adaptations to match these metabolic demands. It might be expected that nutrient supply, digestion and absorption would also be adapted to ensure adequate supply of raw materials for energy production. In short, anatomical and physiological adaptations might be anticipated within the intestinal tract.

Carnivores and herbivores of the same vertebrate class tend to differ in intestinal length and transport rates. Herbivores tend to have longer intestines and higher glucose transport rates (Karasov & Diamond, 1983). The chiropteran intestine has some unusual structural and functional features. In some species, the colon (Okon, 1977; Makanya & Maina, 1994) and external landmarks for locating the foregut–hindgut boundary (Mathis, 1928; Okon, 1977; Madkour et al. 1982) are absent. The unique topography of the intestinal mucosa has also been highlighted (Stutz & Ziswiler, 1984; Makanya & Maina, 1994). Physiological studies indicate that gut transit times may be very short (Klite, 1965; Morrisson, 1980) and certain

Correspondence to Dr Andrew Makanya, Department of Veterinary Anatomy, University of Nairobi, P.O. Box 30197, Nairobi, Kenya.

active transport mechanisms may be lacking (Keegan, 1980; Keegan et al. 1980). Despite this, sugars are absorbed at rates 3 or 4 times faster than in rat intestine (Keegan, 1977). Keegan & Modinger (1979) attributed this high activity in one fruit bat to the presence of a large mucosal surface area and epithelial cells well-endowed with microvilli. However, there are few quantitative data for the villous and microvillous surfaces of bat intestines, in contrast to those of hens and rats (Mayhew, 1990; Elbrønd et al. 1991; Mayhew et al. 1992; Williams & Mayhew, 1992). Consequently, relationships between gut morphology and diet are unclear.

This study provides methods for quantifying the surface features of the chiropteran small intestine. It supplements an earlier qualitative investigation (Makanya & Maina, 1994) in which we established criteria for identifying the boundary between large and small intestines. The quantitative approach relies on randomised (design-based) tissue sampling and uses stereological methods comparable to those applied to the avian coprodaeum (Mayhew et al. 1990). The methods are generally superior to model-based estimates which have proved valuable, under certain circumstances, for analysing villi and microvilli in rat small intestine (Mayhew, 1984, 1987, 1988, 1990; Mayhew & Middleton, 1985; Williams & Mayhew, 1992).

MATERIALS AND METHODS

Three species of bats belonging to 2 suborders were employed. A detailed account of the capture methods is available in Kunz & Kurta (1988). The methods were harmless (provided bats were removed soon after trapping) and applied under the guidance of experts from the National Museums of Kenya who had the necessary permits to capture animals.

To represent Megachiroptera, 10 individuals were sampled. Five epauletted fruit bats (*Epomophorus wahlbergi*, Halowell, 1846) were caught in forests in and around Nairobi and 5 Angola fruit bats (*Lisonycteris angolensis*, Eisentraut, 1965) were obtained from Kakamega (Kenya) by spreading mist nets next to small streams. Bats became entangled in the nets as they descended on the streams to drink water at dusk.

To represent Microchiroptera, 5 longfingered insectivorous bats (*Miniopterus inflatus*, Sanborn, 1936) were caught in Naivasha (Kenya) during the day by spreading a mist net at the cave entrance and stirring the bats from their roosts.

In order to illustrate the sampling and estimation methods, 3 bats were chosen, one individual to represent each of the 3 species. All specimens were male.

Preparation of tissue

Bats were killed by intraperitoneal injection of sodium pentobarbital (50 mg/kg body weight) and the abdominal cavity opened using a ventromedian incision. The oesophagus was severed cranial to the diaphragm and the pelvic bones were carefully cut to reveal the rectum. The entire gastrointestinal tract was dissected free of mesenteries and transferred immediately to a bath of 0.85% sodium chloride. It was opened by a longitudinal incision along the mesenteric border and ingesta/digesta were washed off with fresh saline.

The junction between foregut (= small intestine) and hindgut was identified. In the fruit bat, this junction was observable only on the mucosal aspect being visible as the line of origin of longitudinal colonic folds. In the entomophagous bat, the junction was taken to be the site where intestinal diameter began to increase (a few millimetres cranial to the anus).

Tissue sampling protocol

This is illustrated in Figure 1. After washing, the unstretched lengths of the intestine and parts thereof were measured. This was performed by laying a transparent plastic ruler on the luminal surface of the opened intestine and pressing gently in order to flatten it. The foregut was isolated by severing the foregut–hindgut junction and divided into 5 segments of roughly equal length. The average width and length of each segment was determined before dividing it into 5 approximately equal subsegments. One subsegment from each set was picked at random to represent the segment as a whole and processed for TEM.

Within 4–5 min of death, subsegments were fixed in 2.5% phosphate-buffered glutaraldehyde (pH 7.3) for at least 4 h. Subsegments were washed 3 times in 0.1 M phosphate buffer, postfixed in 1% osmium tetroxide, dehydrated through ascending concentrations of acetone and embedded in Transmit resin (Taab, UK). Before embedding, each piece was placed at the centre of a Petri dish lying on a square test lattice. Next, the Petri dish was spun about its centre so as to randomise the orientation between the subsegment and the 'horizontal' and 'vertical' lines of the lattice. On the toss of a coin, one set of lines (horizontal or vertical) determined the direction in which the microtome knife edge would cut the tissue. The subsegment was embedded so as to satisfy this constraint. This procedure ensured that vertical

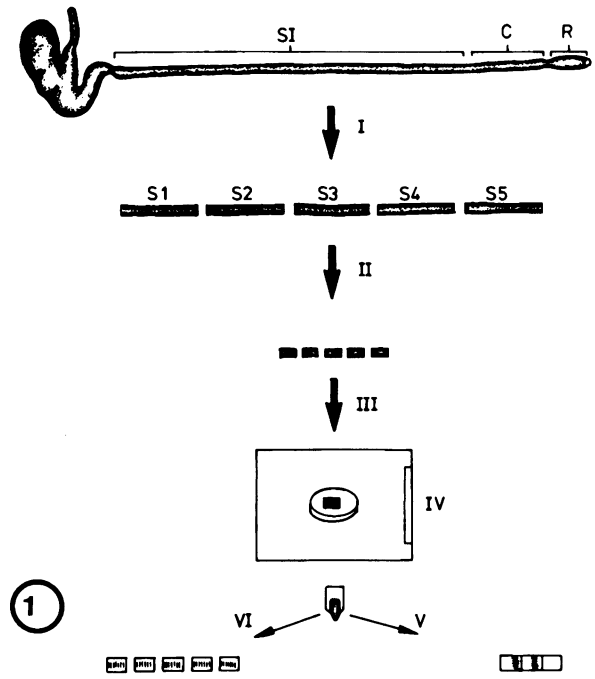

Fig. 1. Schematic drawing of the intestine of the fruit bat and the steps employed in sampling. The intestine comprises small intestine (SI), colon (C) and rectum (R). The SI is sampled after separating it from the rest of the gut and opening it into a flat sheet. It is divided into 5 segments of roughly equal length (see S1-S5 at I) and the average width of each is determined. Each segment is further divided into 5 smaller subsegments (II) which are processed for TEM. One subsegment per set is picked at random (III), placed near the centre of a Petri dish (IV) and spun so as to define a direction for embedding and sectioning. LM and TEM fields (V and VI) are sampled for stereological analysis.

sections of the intestine were isotropic on the reference plane (i.e. the workbench surface). A detailed description and justification of the vertical sectioning method is given in Baddeley et al. (1986). Briefly, vertical sectioning satisfies sampling requirements for unbiased estimation of surface areas.

Vertical sections were studied by LM (nominal section thickness 1 μm) and TEM (measured thickness ~ 60 nm). LM sections were viewed using Nikon or Carl Zeiss optical microscopes. Two toluidine blue-stained sections per segment were prepared and micrographs printed at final linear magnifications of ×80 (frugivorous bats) and ×100 (insectivorous bats). Ultrathin sections were viewed using Philips EM 300 or EM 410 microscopes operated at 80 kV accelerating voltage. For analyses at TEM levels, about 5 micrographs per segment were prepared at final magnifications of ×18500 (fruit-eaters) and ×50000 (insect-eaters).

Stereological methods

We adopted a multilevel sampling scheme (Cruz-Orive & Weibel, 1981) with 3 levels of estimation, each level representing a given magnification stage. *Level 1.* Macroscopic estimates of a reference surface, here that of the unmodified mucosal tube (primary mucosa) in a given segment—symbol S(pm). *Level 2.* LM estimates of the extent to which villi amplify the surface of the primary mucosa—ratio S(v)/S(pm). *Level* 3. TEM estimates of the extent to which microvilli amplify the surface area of villi—ratio S(mv)/S(v). The surface area of villi in a segment is given by

$$S(v) = S(pm) \times S(v)/S(pm)$$

and the surface area of microvilli by

$$S(mv) = S(pm) \times S(v)/S(pm) \times S(mv)/S(v)$$

where the 3 variables on the right-hand side represent estimates obtained at levels 1, 2 and 3 respectively.

The surfaces in an entire intestine are estimated merely by summing the values obtained in individual segments. For instance, the absolute surface area of microvilli per whole intestine (5 segments in total) was estimated as

$$S(mv)t = S(mv)1 + S(mv)2 + S(mv)3 + S(mv)4 + S(mv)5.$$

In multilevel sampling schemes, it is important to maintain consistency of definition for a given feature when moving from one magnification level to another (Cruz-Orive & Weibel, 1981). In this study, a small bias has been introduced by equating the apical border of epithelial cells (level 3) with the apical plasmalemma in microvillus-free regions and the surface containing the bases of microvilli in other regions (Mayhew et al. 1990). This boundary might not be so easily resolved at level 2 where the villous surface was being identified.

Level 1 analyses. The primary surface area was estimated by multiplying the average internal circumference of each intestinal segment (c) by the length (l) of the segment:

$$S(pm) = c \times l.$$

Level 2 analyses. On LM fields of view, lattices of cycloid test lines were superimposed so as to be random in position but with the vertical directions of the tissue and lattice running in parallel (Baddeley et al. 1986). Intersections were counted between the test lines and profiles of the villi, I(v), on the one hand and those of the primary mucosal surface, I(pm), on the other. The primary mucosal surface was taken to be the interface running between the bases of villi and the openings of crypts. I(v) and I(pm) were summed for each segment and the totals provided the intersection ratio, I(v)/I(pm).

The villous amplification factor, S(v)/S(pm), was taken to be numerically equal to the intersection ratio, I(v)/I(pm), and the villous surface area per intestinal segment was estimated as

$$S(v) = S(pm) \times I(v)/I(pm).$$

Level 3 analyses. At TEM levels, intersections were counted between cycloid test lines and the traces of microvilli, I(mv), and the apical epitheliocyte membrane, I(em). The apical membrane was taken to be the interface running at the level of the bases of microvilli. Total intersection counts on TEM fields of view, I(mv) and I(em), were obtained for each segment and microvillous amplification factor, S(mv)/S(v), computed directly from the intersection ratio.

Other useful quantities (*Level* 3). These comprised estimates of the sizes and numbers of microvilli. (1) *Microvillous diameter, d(mv).* This was estimated by measuring the diameters of at least 10 favourably sectioned microvilli and computing the average across all micrographs representing a given segment. If a microvillus was cut obliquely, the short axis of its profile was measured. (2) *Microvillous height, h(mv).* The mean height of microvilli in a given segment was estimated by measuring the profiles of at least 30 microvilli sectioned along their long axes. The presence of clear (nonfuzzy) lateral plasmalemma traces was taken to indicate that a microvillus was sectioned longitudinally. (3) *Surface of the average microvillus, s(mv).* This was computed on a per segment basis (see Mayhew, 1990) using the formula, $s(mv) = \pi \times d(mv) \times h(mv)$. (4) *Packing density of microvilli, N(mv)/S(v).* This is the number of microvilli per unit surface area of apical cell membrane and was estimated (Mayhew, 1990) by

$$N(mv)/S(v) = [S(mv)/S(v)]/s(mv).$$

(5) *Total number of microvilli, N(mv).* Estimated by dividing the total surface of microvilli by the surface of the average microvillus in the same segment. Segmental values were summed in order to calculate values per intestine.

A worked example

One of the bats possessed an intestine of length $L =$ 180 mm and, therefore, the average segment length was $L/5 = l = 36$ mm. The average circumference of the first segment from the same intestine was $c = 5.5$ mm. *Level 1.* The estimated primary mucosal surface area of this segment was

$$S(pm)1 = 5.5 \times 36 = 198 \text{ mm}^2.$$

This was repeated for all other segments once values of c were known.

Level 2. The total numbers of intersections between surface traces and cycloid arcs were counted using 2 superimpositions on the same fields and were I(pm) = 12 and I(v) = 84. From these data, the villous amplification factor was calculated to be $84/12 = 7.00$ and the absolute villous surface to be

$$S(v)1 = 198 \times 7.00 = 1386 \text{ mm}^2.$$

Level 3. For 2 (microvilli) and 5 (epithelial cell apical border) superimpositions on the same fields, the numbers of intersections between membranes and cycloid arcs were I(mv) = 589 and I(em) = 49. Therefore, the microvillous amplification factor was $(589 \times 5)/(49 \times 2) = 30.05$ and absolute microvillous surface area was

$$S(mv)1 = 1386 \times 30.05 = 41650 \text{ mm}^2.$$

These values are not corrected for image overprojection effects dependent upon section thickness (Gundersen, 1979; Weibel, 1979; Mayhew, 1983).

In the same segment, the mean diameter of microvilli was 99.8 nm and mean length was 1.10 μm from which mean surface was calculated to be 0.3449 μm^2. Consequently, the packing density of microvilli was $30.05/0.3449 = 87.1$ microvilli per μm^2 of cell surface and the uncorrected total number of microvilli in that segment was

$$N(mv)1 = (41650 \times 10^6)/0.3449 = 1.21 \times 10^{11}.$$

Total surfaces. The above steps were repeated for other segments and the following microvillous areas were obtained: $S(mv)2 = 32950 \text{ mm}^2$, $S(mv)3 = 17390 \text{ mm}^2$, $S(mv)4 = 8515 \text{ mm}^2$ and $S(mv)5 = 8771 \text{ mm}^2$. The total surface in the entire intestine amounted to

$$S(mv)t = 109300 \text{ mm}^2 \text{ or } 0.11 \text{ m}^2.$$

RESULTS

Body weights and intestinal lengths are given in Table 1. The 3 bats (1 = *M. inflatus*, 2 = *E. wahlbergi* and 3 = *L. angolensis*) weighed 8.98, 68.83 and 75.80 g respectively. Corresponding intestinal lengths were 180, 600 and 650 mm.

Table 1. *Body weight and foregut length in representatives of three species of bat*

	Bat number*		
Variable	1	2	3
Body weight (g)	8.98	68.83	75.80
Gut length (mm)	180	600	650

* Numbers refer to the following species: 1, *Miniopterus inflatus*; 2, *Epomophorus wahlbergi*; 3, *Lisonycteris angolensis.*

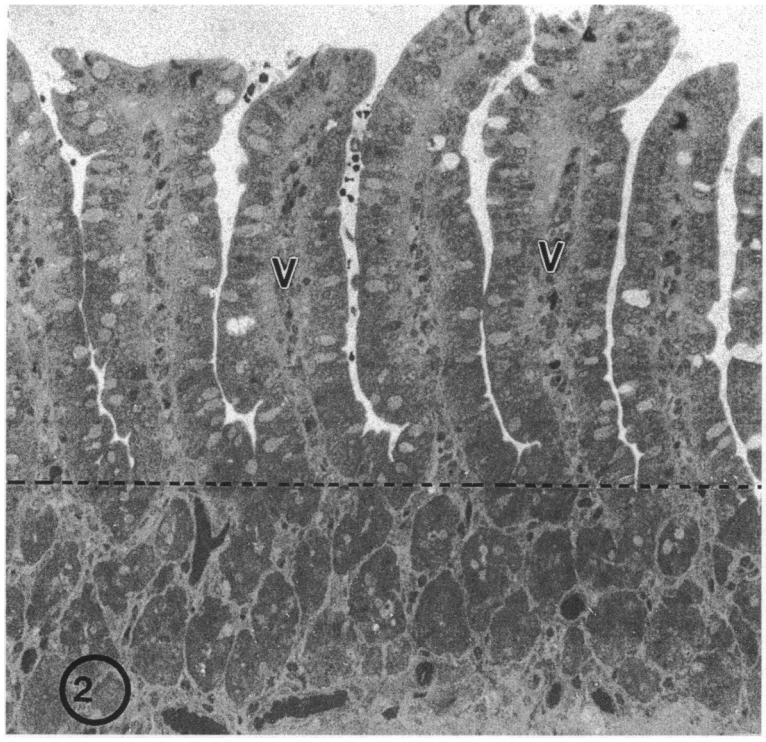

Fig. 2. LM appearance of the small intestine of the entomophagous bat, *Miniopterus inflatus*. The close packing of villi (V) is partly responsible for the surface amplification estimated at Level 2. The hatched line represents the crypt–villus interface which is used for estimating the test intersections with the surface of primary mucosa, I(pm). Toluidine blue, × 200.

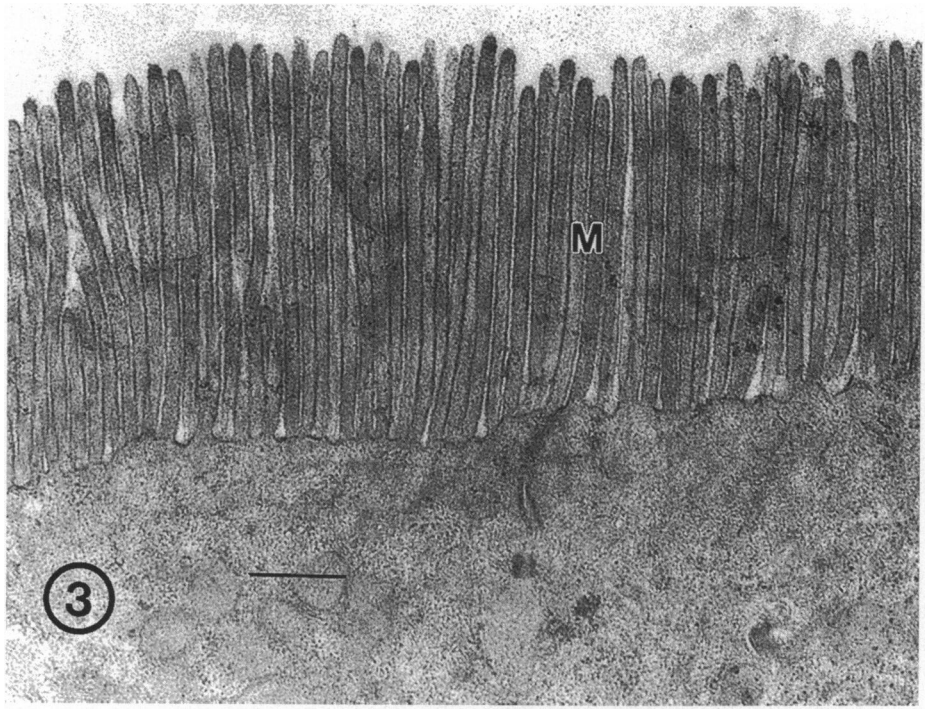

Fig. 3. Ultrastructural appearance (Level 3) of microvilli (M) at the apical surface of enterocytes of a fruit bat, *Lisonycteris angolensis*. The vertical direction at this level is defined by a perpendicular to the epithelial basal lamina. Lead citrate and uranyl acetate. Bar, 0.8 μm.

The LM morphology of the first segment of the foregut of the insectivorous bat (*M. inflatus*) is illustrated in Figure 2. It shows a tightly packed arrangement of villi responsible for the villous amplification factor computed at level 2. The ultrastructural appearance of microvilli at the apical border of villous enterocytes (level 3) is indicated in Figure 3.

Morphometric findings are summarised in Tables

Table 2. *Circumference and relative and absolute surface areas in the foregut of three species of bat*

Variable	Bat no.	Gut segment 1	2	3	4	5
c, mm	1	5.5	5.0	5.0	4.0	4.0
	2	12.0	9.0	10.0	8.0	5.0
	3	8.0	7.0	5.0	5.0	5.0
S(pm), mm^2	1	198	180	162	144	144
	2	1440	1080	1200	960	600
	3	1040	910	650	650	650
S(v)/S(pm), mm^2/mm^2	1	7.0	7.0	6.0	3.0	2.7
	2	11.8	8.4	7.5	4.3	3.0
	3	8.7	6.7	6.0	4.7	2.5
S(v), mm^2	1	1386	1260	972	432	389
	2	16990	9072	9000	4128	1800
	3	9048	6097	3900	3055	1625
S(mv)/S(v), mm^2/mm^2	1	30.1	26.2	17.9	19.7	22.6
	2	46.7	39.8	35.1	39.3	33.1
	3	47.9	33.4	49.6	40.6	33.7
S(mv), cm^2	1	416	329	174	85	88
	2	7933	3609	3160	1624	595
	3	4337	2037	1933	1240	547

Table 3. *Dimensions and numbers of microvilli in the foregut of three species of bat*

Variable	Bat no.	Gut segment 1	2	3	4	5
d(mv), nm	1	100	80	80	80	93
	2	108	97	81	81	87
	3	127	108	106	108	126
h(mv), μm	1	1.10	0.81	0.75	0.79	0.82
	2	2.70	2.47	2.05	2.05	2.70
	3	4.23	3.78	3.17	1.95	1.47
s(mv), μm^2	1	0.34	0.20	0.19	0.20	0.24
	2	0.91	0.75	0.52	0.52	0.74
	3	1.69	1.28	1.06	0.66	0.58
N(mv)/S(v), μm^{-2}	1	87	128	95	100	94
	2	51	53	67	75	45
	3	28	26	47	61	58
N(mv), $\times 10^{11}$	1	1.21	1.61	0.93	0.43	0.36
	2	8.66	4.79	6.06	3.11	0.81
	3	2.57	1.59	1.83	1.87	0.94

1–3. In all animals there appeared to be gradients of intestinal morphology with greater values of intestinal circumference and surface areas (Table 2) and microvillous number (Table 3) in more proximal segments.

For the entire intestine, the mean circumference was 4.6 mm (bat 1), 8.8 mm (bat 2) and 6.0 mm (bat 3). Mean amplification factors for villi were 5.4, 7.8 and 6.1, and those for microvilli were 25, 41 and 43 respectively. The estimated primary mucosal surface areas of the entire small intestine were 8.3, 52.8 and 39.0 cm^2 whilst corresponding villous surface areas were 44.4, 410 and 237 cm^2. Uncorrected microvillous surfaces were 0.11, 1.69 and 1.01 m^2 whilst numbers were 4.5×10^{11}, 23.4×10^{11} and 8.8×10^{11} respectively.

Mean microvillous diameters per intestine varied from 88 to 115 nm, heights from 0.88 to 3.15 μm and mean areas from 0.24 to 1.11 μm^2. On average, they were packed on the cell apex at densities of 102, 57 and 37 per μm^2 respectively.

When normalised for body weight, the quantitative results indicate relative villous surfaces of 3.1, 6.0 and 4.9 cm^2/g and uncorrected microvillous surfaces of 122, 246 and 133 cm^2/g.

DISCUSSION

A procedure has been produced for estimating the functional surfaces of bat small intestines with reasonable efficiency and minimal biases. After design-based sampling, surface estimation was undertaken by using vertical sections with cycloid test lines (Baddeley et al. 1986).

The results are not entirely free of some of the technical biases associated with quantifying sampled tissue sections. One such bias, tissue processing distortion, is of minimal concern because glutaraldehyde fixation and resin embedding introduce little distortion (Hayat, 1981; Burton & Palmer, 1988); nor has bias introduced by the Holmes or overprojection effect (Gundersen, 1979; Weibel, 1979; Mayhew, 1983) been corrected in this study. Its magnitude varies with section thickness and object size but it has little impact on villous surface area since villi are large compared to section thickness. However, microvillous amplification factors may be overestimated due to the relatively small dimensions of these organelles (Gundersen, 1979; Mayhew et al. 1990). The overall error can be estimated using the length and diameter averaged over all microvilli in the entire intestine and taking the mean section thickness of 60 nm. On this basis, the relative biases would amount to 51% (bat 1), 43% (bat 2) and 35% (bat 3) but these are only approximations because microvilli seem to vary in length, diameter and number in different segments and different species. With the average dimensions shown in Table 3, the segmental biases are likely to be 44–56% (bat 1), 38–50% (bat 2) and 31–38% (bat 3). In the rat small intestine, the bias within a segment was found to be 34–54% for a section thickness of 70 nm (Mayhew & Middleton, 1985; Mayhew, 1987).

Further bias may arise because of problems associated with organ identification. In the bat, the boundary between small and large intestines can be difficult to identify since neither caecum nor appendix

is present and the external characteristics of small and large intestines are similar (Mathis, 1928; Okon, 1977; Madkour et al. 1982). In fruit bats, the boundary was taken to be where the macroscopic longitudinal folds of the colon began. The absence of a colon in insectivores was noted first by Okon (1977). Although a colon has been defined in one entomophagous bat (Ishikawa et al. 1985), our studies (Makanya & Maina, 1994) have provided no anatomical evidence of its presence. In contrast, the rectum in insect-eaters is conspicuous on account of its greater diameter (Makanya & Maina, 1994).

The present study was prompted by a desire to compare intestinal morphology in bats with different lifestyles. Now that a reproducible protocol is available, this will be the subject of future investigations. So far, it appears that differences between bats are achieved by adaptations at several levels of structural organisation. These include increases in intestinal length and circumference, villous amplification and microvillous amplification. The latter seems to be effected mainly by disproportionate alterations in the length of microvilli, although diameters may also alter with consequent changes in packing densities. In birds and rodents, microvillous elongation is part of the process of enterocyte maturation as cells migrate along the crypt–villus axis (Brown, 1962; van Dongen et al. 1976; Stenling & Helander, 1981; Smith & Brown, 1989) and a feature of variation in cell morphology along the intestine (Mayhew, 1990). In avian coprodaeum, the length and packing density of microvilli vary with dietary salt load (Mayhew et al. 1992). In rats and hamsters, length may also vary during adaptation to reduced food intake (Misch et al. 1980; Buschmann & Manke, 1981*a*, *b*; Mayhew, 1987) but not in response to experimental diabetes (Mayhew, 1990). Changes in absorptive surface areas in the avian coprodaeum and rodent small intestine are also effected by cell recruitment onto villi. The extent to which this explains species differences in surface areas in chiroptera is unknown.

The packing densities and linear dimensions of microvilli vary between bats and rats. In the present study, the mean length of microvillus per intestine was 0.88–3.15 μm, mean diameter 88–115 nm and packing density 37–102 per μm^2. In rats, microvilli tend to be shorter (1.2–1.4 μm), slightly thicker (106–127 nm) and less densely packed (34–43 per μm^2; see Mayhew, 1990). Despite these differences, absolute microvillous surface area in these bats is not much lower than that in rat small intestine (0.1–1.2 m^2 versus 0.9–1.2 m^2 after correcting for section thickness bias; see Mayhew & Middleton, 1985; Mayhew, 1990). However, when normalised for body weight, the relative surface areas of microvilli are much greater in the bat (81–172 cm^2/g in bats versus 14–42 cm^2/g in rats; Mayhew, 1990).

ACKNOWLEDGEMENTS

These studies were supported by The World Bank and the Deans' Committee of the University of Nairobi. We are grateful to Joseph Kwambai for providing the specimens on which the study is based, and to Alan Pyper, Tim Self, Barry Shaw and Amos Tangai for excellent technical assistance.

REFERENCES

AYETTEY AS, TAGOE CNB, YATES RD (1991) Morphometric study of the ventricular myocardial cells in the bat (*Pipistrellus pipistrellus*), hamster (*Mesocricetus auratus*) and Wistar rat. *Acta Anatomica* **141**, 348–351.

BADDELEY AJ, GUNDERSEN HJG, CRUZ-ORIVE LM (1986) Estimation of surface area from vertical sections. *Journal of Microscopy* **142**, 259–276.

BROWN AL (1962) Microvilli of the human jejunal epithelial cell. *Journal of Cell Biology* **12**, 623–627.

BURTON GJ, PALMER ME (1988) Eradicating fetomaternal fluid shift during perfusion fixation of human placenta. *Placenta* **9**, 327–332.

BUSCHMANN RJ, MANKE DJ (1981*a*) Morphometric analysis of the membranes and organelles of small intestinal enterocytes. I. Fasted hamster. *Journal of Ultrastructure Research* **76**, 1–14.

BUSCHMANN RJ, MANKE DJ (1981*b*) Morphometric analysis of the membranes and organelles of small intestinal enterocytes. II. Lipid-fed hamster. *Journal of Ultrastructure Research* **76**, 15–26.

CARPENTER RE (1975) Flight metabolism of flying foxes. In *Swimming and Flying in Nature*, vol. 2 (ed. C. J. Brokaw & C. Brennen), pp. 883–890. New York: Plenum.

CRUZ-ORIVE LM, WEIBEL ER (1981) Sampling designs for stereology. *Journal of Microscopy* **122**, 235–257.

DAWSON RW (1975) Avian physiology. *Annals of Reviews of Physiology* **37**, 441–465.

ELBRØND VS, DANTZER V, MAYHEW TM, SKADHAUGE E (1991) Avian lower intestine adapts to dietary salt (NaCl) depletion by increasing transepithelial sodium transport and microvillous membrane surface area. *Experimental Physiology* **76**, 733–744.

GREENHALL AM, PARADISO JD (1968) *Bats and Bat Banding*. Washington, DC: Bureau of Sport, Fisheries & Wildlife Resource Publication 72.

GUNDERSEN HJG (1979) Estimation of tubule or cylinder L_v, S_v and V_v on thick sections. *Journal of Microscopy* **117**, 333–345.

HAYAT MA (1981) *Fixation for Electron Microscopy*. New York: Academic Press.

ISHIKAWA OK, MATOBA M, TANAKA H, ONO K (1985) Anatomical study of the intestine of the insect-feeder bat *Myotis frater kaguae*. *Journal of Anatomy* **142**, 141–150.

JURGENS DK, BARTELS H, BARTELS R (1981) Blood oxygen transport and organ weights of small bats and non-flying mammals. *Respiration Physiology* **45**, 243–260.

KARASOV WH, DIAMOND JM (1983) Adaptive regulation of sugar and amino acid transport by vertebrate intestine. *American Journal of Physiology* **245**, G443–G462.

KEEGAN DJ (1977) Aspects of assimilation of sugars by Rousettus aegypticus. *Comparative Biochemistry and Physiology* **58A**, 349–352.

KEEGAN DJ (1980) Lack of active glucose transport system in the bat, Rousettus aegypticus, intestine. *South African Journal of Science* **76**, 570–571.

KEEGAN DJ, MODINGER R (1979) Microvilli of the intestinal mucosal cells of the bat, Rousettus aegypticus. *South African Journal of Zoology* **14**, 220–223.

KEEGAN DJ, LEVINE S, BALGOBIND ND (1980) Absorption of calcium in the small intestine of the bat, Rousettus aegypticus. *South African Journal of Science* **76**, 328.

KLITE PD (1965) Intestinal bacterial flora and transit time in three neotropical bat species. *Journal of Bacteriology* **90**, 375–379.

KUNZ TH, KURTA A (1988) Capture methods and holding devices. In *Ecological and Behavioural Methods for the Study of Bats* (ed. T. H. Kunz). Washington DC; London: Smithsonian Institution Press.

MADKOUR GA, HAMMOUDA EM, IBRAHIM JG (1982) Histology of the alimentary tract of two common Egyptian bats. *Annals of Zoology (Agra)* **19**, 53–73.

MAINA JN, KING AS, KING DZ (1982) A morphometric analysis of the lung of a species of bat. *Respiration Physiology* **50**, 1–11.

MAINA JN, THOMAS SP, HYDE DM (1991) A morphometric study of the lungs of different sized bats: correlations between structure and function of the chiropteran lung. *Philosophical Transactions of the Royal Society of London* B **333**, 31–50.

MAKANYA AN, MAINA JN (1994) Morphology of the alimentary tract of the insectivorous Horseshoe bat, *Rhinolophus hildebrandti*, Peters: a scanning and light microscopic study. *African Journal of Ecology* **32**, 158–168.

MATHIS J (1928) Beitrag zur Kenntris des fleder Mausdermes. *Zeitschrift für Zellforschung* **8**, 595–647.

MAYHEW TM (1983) Stereology: progress in quantitative microscopical anatomy. In *Progress in Anatomy, Volume 3* (ed. V. Navaratnam & R. J. Harrison), pp. 81–112. Cambridge: Cambridge University Press.

MAYHEW TM (1984) Geometric model of the rat intestinal mucosa for the stereological evaluation of villus amplification factors. *Journal of Microscopy* **135**, 337–346.

MAYHEW TM (1987) Quantitative ultrastructural study on the responses of microvilli along the small bowel to fasting. *Journal of Anatomy* **154**, 237–243.

MAYHEW TM (1988) Geometric model for estimating villous surface area in the rat small bowel is justified by unbiased estimates obtained using vertical sections. *Journal of Anatomy* **161**, 187–193.

MAYHEW TM (1990) Striated brush border of intestinal absorptive epithelial cells: stereological studies on microvillous morphology in different adaptive states. *Journal of Electron Microscopy Technique* **16**, 45–55.

MAYHEW TM, MIDDLETON C (1985) Crypts, villi and microvilli in the small intestine of the rat. A stereological study of their variation within and between animals. *Journal of Anatomy* **141**, 1–17.

MAYHEW TM, DANTZER V, ELBRØND VS, SKADHAUGE E (1990) A sampling scheme intended for tandem measurements of sodium transport and microvillous surface area in the coprodaeal epithelium of hens on high- and low-salt diets. *Journal of Anatomy* **173**, 19–31.

MAYHEW TM, ELBRØND VS, DANTZER V, SKADHAUGE E (1992) Quantitative analysis of factors contributing to expansion of microvillous surface area in the coprodaeum of hens transferred to a low-NaCl diet. *Journal of Anatomy* **181**, 73–77.

MISCH DW, GIEBEL PE, FAUST RG (1980) Intestinal microvilli: responses to feeding and fasting. *European Journal of Cell Biology* **21**, 269–279.

MORRISSON DW (1980) Efficiency of food utilization by fruit bats. *Oecologia* **45**, 270–273.

OKON EE (1977) Functional anatomy of the alimentary canal in the fruit bat Eidolon helvum and the insect bat Tadarida nigeriae. *Acta Zoologica (Stockholm)* **58**, 83–93.

SMITH MW, BROWN D (1989) Dual control over microvillus elongation during enterocyte development. *Comparative Biochemistry and Physiology* **93A**, 623–628.

STENLING R, HELANDER HF (1981) Stereologic studies on the small intestinal epithelium of the rat. 1. The absorptive cells of the normal duodenum and jejunum. *Cell and Tissue Research* **217**, 11–21.

STUTZ H, ZISWILER V (1984) Morphological and histological investigations of the digestive tract of the middle European bats (Mammalia: Chiroptera). *Myotis* **21/22**, 41–46.

THOMAS DW (1984) Fruit intake and energy budgets of frugivorous bats. *Physiological Zoology* **57**, 457–467.

THOMAS SP (1975) Metabolism during flight in two species of bats, *Phyllostomus hastatus* and *Pteropus gouldii*. *Journal of Experimental Biology* **63**, 273–293.

THOMAS SP (1980) The physiology and energetics of bat flight. In *Proceedings of the Fifth International Bat Research Conference* (ed. D. W. Wilson & A. Galdner), pp. 393–402. Lubbock, Texas: Texas Technical Press.

THOMAS SP, SUTHERS RA (1972) The physiology and energetics of bat flight. *Journal of Experimental Biology* **57**, 317–335.

TUCKER VA (1972) Respiration during flight in birds. *Respiration Physiology* **14**, 75–82.

VAN DONGEN JM, VISSER WJ, DAEMS WTH, GALJAARD H (1976) The relation between cell proliferation, differentiation and ultrastructural development in rat intestinal epithelium. *Cell and Tissue Research* **174**, 183–199.

WEIBEL ER (1979) *Stereological Methods*, vol. 1, *Practical Methods for Biological Morphometry*. New York: Academic Press.

WILLIAMS M, MAYHEW TM (1992) Responses of enterocyte microvilli in experimental diabetes to insulin and an aldose reductase inhibitor (ponalrestat). *Virchows Archiv, B Cell Pathology* **62**, 385–389.

WIMSATT WA (1970) *Biology of Bats*, vol. 1. New York, London: Academic Press.

YALDEN DW, MORRIS PA (1975) *The Lives of Bats*. Vancouver: New York Times Book Co.